Article

Modified Alginate-Based Hydrogel as a Carrier of the CB2 Agonist JWH133 for Bone Engineering

Wei Zhou,[†] Qianming Li,[†] Ruixiang Ma,[†] Wei Huang, Xianzuo Zhang, Yingsheng Liu, Ze Xu, Linlin Zhang, Meng Li,* and Chen Zhu*

Read Online

ACCESS | Metrics & More | Article Recommendations

ABSTRACT: Alginate hydrogels have been widely used as excellent scaffold materials for implantation in biological systems because of their good biocompatibility. However, it is difficult to repair bone defects with these materials because of their poor mechanical properties. The aim of the present study was to fabricate a novel degradable alginate/palygorskite (PAL) composite hydrogel with good mechanical properties and investigate its potential for application in bone defect repair. The modified alginate-based hydrogel with increasing PAL content exhibited better mechanical properties than the original alginate hydrogel. In addition, the resulting composite hydrogel was thoroughly characterized by scanning electron microscopy (SEM). With increasing PAL content, the swelling ratio of the hydrogel increased in PBS (pH = 7.4). *In vitro* cytocompatibility was evaluated using bone marrow-derived mesenchymal stem cells (BMSCs) to confirm that the developed composite hydrogel was cytocompatible after 1, 3, and 7 days. All these results suggest that the developed composite hydrogel has great potential for bone tissue engineering applications. JWH133 is a selective agonist of cannabinoid receptor type 2 (CB2), which exerts dual anti-inflammatory and anti-osteoclastogenic effects. We co-cultured BMSCs with composite hydrogels loaded with JWH133, and analysis of proliferation and osteogenic differentiation indicated that the composite hydrogel loaded with JWH133 may enhance the osteogenic differentiation of rat BMSCs. Furthermore, we found that the composite hydrogel loaded with JWH133 inhibited osteoclast formation and the mRNA expression of osteoclast-specific markers. In summary, the developed composite hydrogel has a high drug-loading capacity, good biocompatibility, and strong potential as a drug carrier for treating osteoporosis by promoting osteoblast and inhibiting osteoclast formation and function.
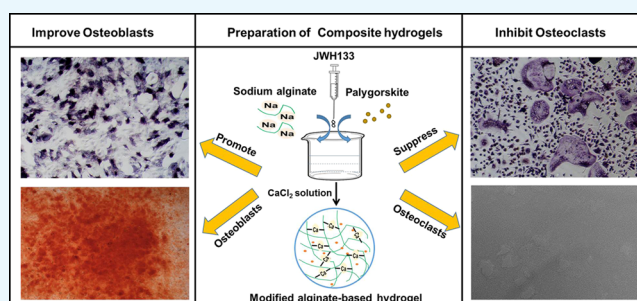
INTRODUCTION

Bone defects are common orthopedic conditions that are often caused by high-energy impact or trauma, tumor resection, infection, or revision surgery.[1−3] Bone defects are especially common among elderly patients, who often suffer from osteoporosis because of a reduction in bone mass.[4,5] The characteristics of osteoporosis include low bone mass and micro-architectural deterioration of the bone caused by more rapid bone resorption than new bone formation, which usually leads to fragile bone and an increased risk of fracture.[6−8] The treatment of osteoporotic fractures, especially osteoporotic fractures with bone defects, remains a critical challenge. Mild bone defects can self-heal, but if the area of the defect is large, healing will be difficult and require adjuvant therapy. Bone grafting is a traditional clinical method used to repair bone defects, but there are a number of potential risks and complications.[9,10] With the development of tissue engineering technology, treatment methods for bone defects have greatly improved. At present, bone substitute materials, such as porous collagen matrices, synthetic polymeric porous blocks, and injectable polymeric hydrogels,[11−13] have achieved some success in addressing the shortcomings of traditional therapies and yielding better results in the field of bone regeneration. Ideal bone substitute materials should have a three-dimensional porous structure, appropriate mechanical strength, biodegradability, biocompatibility, and osteoinductive ability.[14−16] Any single material has difficulty meeting the repair requirements, and composite materials have become a research focus in the treatment of osteoporotic bone defects.

Hydrogels, such as those composed of sodium alginate (SA),[17,18] collagen (COL), and agarose (AG),[19] have potential as scaffolds for tissue engineering because of their excellent biocompatibility, degradability, and similarities to the natural
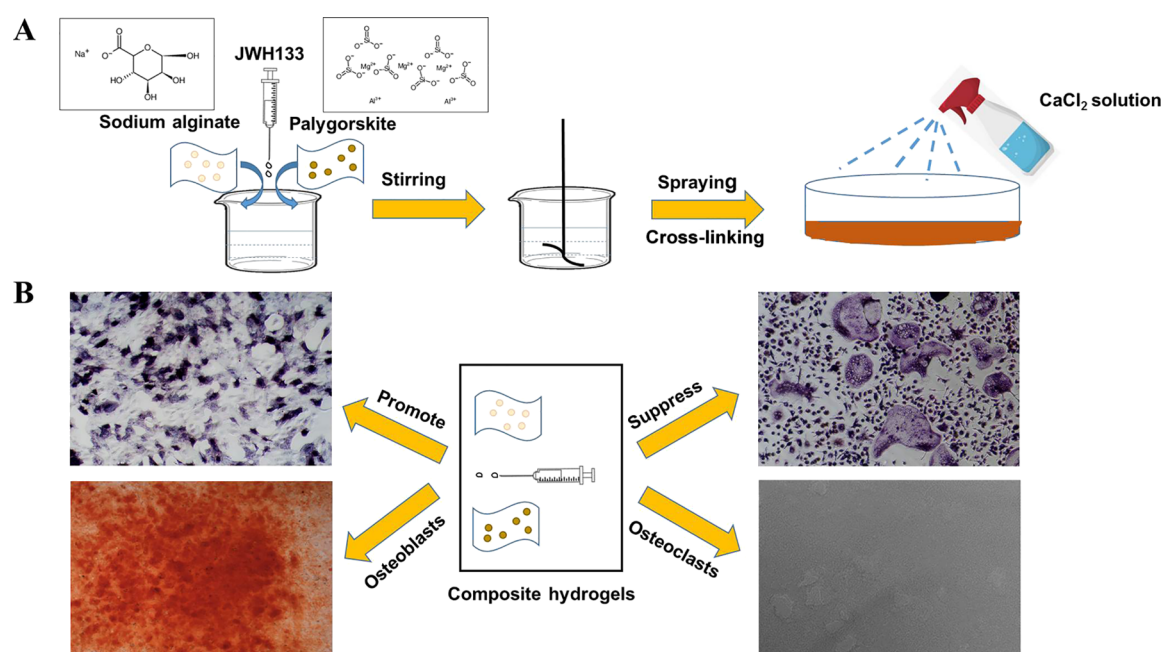
Figure 1. Schematic diagram of crosslinking technology to generate the composite hydrogel (A), which promotes osteogenesis and suppresses osteoclastogenesis (B). Photograph courtesy of Wei Zhou. Copyright 2020.

extracellular matrix, and these materials could provide a three-dimensional support for cellular growth and tissue formation. Alginates belong to a family of linear block polyanionic copolymers composed of (1−4)-linked-D-mannuronic acid (M units) and (1−4)-linked-L-guluronic acid (G units) residues.[20] Alginate can form stable hydrogels in the presence of divalent cations, such as Ca^{2+} and Mg^{2+}, *via* the ionic interaction between the cation and the carboxyl functional group of G units located on the polymer chain.[21] Alginate has a number of advantageous features, including biocompatibility, nonimmunogenicity, and degradability, and has long been used as an excellent scaffold material for implantation in biological systems.[22] Alginate has been widely used as a gelling agent for food products and has become an attractive material for tissue engineering.[23−25] However, alginate hydrogels are difficult to use in bone defect repair because of their poor mechanical properties. In addition, it is difficult for the hydrogel to maintain its original shape and degrade easily, which limits its application alone as a bone repair material. Therefore, improving its mechanical and osteoinductive properties by combination with another material has become an important research topic.

Palygorskite (PAL) is a magnesium aluminum silicate mineral with a hydrated chain-layer structure.[26] PAL can be formed in fibrous single crystals. It has a unique dispersion, high-temperature resistance, alkali resistance, a good adsorption ability, good drug-loading capacity, as well as good biological activity and compatibility.[27,28] Moreover, PAL is composed of SiO_2 (55.03%), Al_2O_3 (10.24%), MgO (10.49%), Fe_2O_3 (3.53%), H_2O^+ (10.13%), and H_2O^- (9.73%), which are in the form of compounds, and will not exist or release as the single ion.[29] PAL has been widely used in many areas but has rarely been used in research on bone tissue engineering. PAL is rich in many elements related to bone formation, including silicon, magnesium, and iron, and some studies have shown that nanofiber loading PAL could improve the ability of osteoblastic.[30,31] Therefore, PAL is suitable for new explorations in bone tissue engineering research.

The process of repairing bone defects is complicated and involves the differentiation and function of osteoblasts and osteoclasts.[32] The metabolism of the bone is a dynamic balance between bone resorption and bone formation, which is regulated by many signaling pathways, including the Wnt/β-catenin, BMP/Smad, MAPK, NF-kB, and PI3K/Akt signaling pathways.[33,34] Under the pathological conditions of osteoporosis, disruption of the bone formation and bone resorption balance results in the poor repair of bone defects.[35] Osteoclasts play an important role in bone resorption by secreting acid and proteases to dissolve mineral components of the bone.[36] Cannabinoid receptor 2 (CB2) has been widely studied for the treatment of inflammatory and osteolytic bone disorders.[37] CB2, which is an important regulator of bone remodeling, affects the differentiation and maturation of bone cells.[38,39] Furthermore, the selective CB2 agonist JWH133 exerts dual anti-inflammatory and anti-osteoclastogenic effects by inhibiting the NF-kB signaling pathway.[40]

In this study, we combined the alginate hydrogel with PAL powder, which was expected to repair bone defects (Figure 1A), provide a certain amount of mechanical support at the damaged site, and promote new bone formation. The research schematic diagram is shown in Figure 1B. We evaluated the mechanical properties of the composite hydrogels with different concentrations of PAL to find the best ratio. Then, the proliferation and differentiation of cells cultured on the co-cross-linked hydrogel was studied. The composite hydrogel showed good mechanical strength, drug-loading capacity, and biocompatibility. Importantly, JWH133 loaded in the composite stimulated BMSC differentiation into osteoblasts but suppressed osteoclast differentiation *in vitro*. This research provides a foundation for new ideas and methods for bone defect reconstruction and expands the practical clinical applications of degradable hydrogel materials in the bone defect repair.
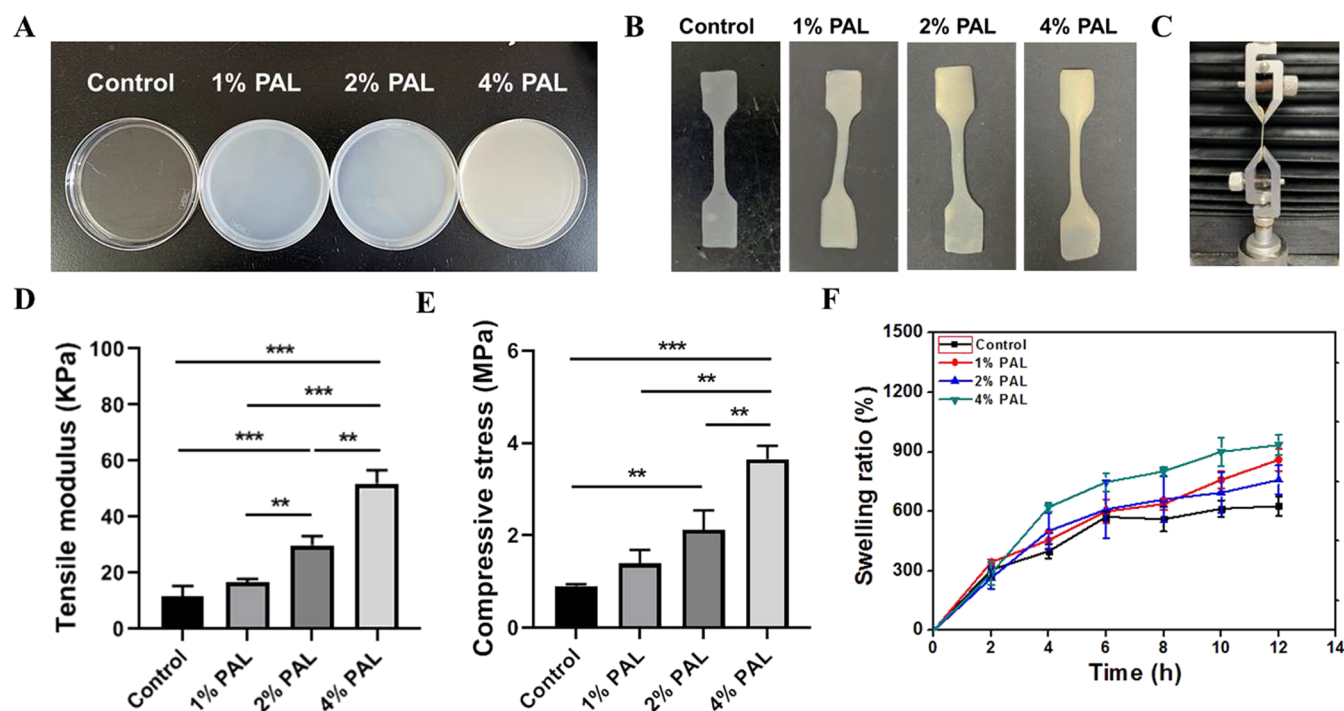
Figure 2. Physical characterization of the composite hydrogel. (A) Homogeneous solution was poured into culture dishes and shaken until evenly dispersed. (B) Samples were cut into dumbbells for the tensile test. (C) Photo showing the setup of the tensile test. (A−C) Photograph courtesy of Wei Zhou. Copyright 2020. (D) Tensile modulus and (E) compressive strength of the composite hydrogel samples, including 1, 2, and 4 w/v % PAL and no PAL as the control group. Data are the mean ± standard deviation ($n = 5$). (F) Swelling ratio of the composite hydrogel samples in PBS (pH = 7.4) at 37 °C.

■ EXPERIMENTAL SECTION

Materials. PAL powder was obtained from Shengyi Nano Technology Co., Ltd., Xuyi City, Jiangsu Province. Sodium alginate (SA) was purchased from Aladdin Chemical Reagent Co., Ltd. (Shanghai, China). The water used in all experiments was double-distilled water. Other chemical agents were analytically pure.

Preparation of Modified Alginate-Based Hydrogel. One gram, two, or four g of PAL powder was dispersed under rapid agitation in 100 mL of deionized water, and no PAL was used as a control group. Different concentrations of clay suspensions (1 w/v %, 2 w/v %, and 4 w/v % PAL) were obtained. Then, JWH133 (Tocris Bioscience, Bristol, UK) was added into the clay suspensions. Finally, 0.3 g of SA was added and dissolved under stirring until a homogeneous solution was obtained. The homogeneous solution was poured into a cell dish (Figure 2A) and shaken until evenly dispersed. Finally, the homogeneous solution was cross-linked with 2 mL of the CaCl$_2$ (100 mM) solution (purchased from Sinopharm Chemical Reagent Co., Ltd., Shanghai, China) at room temperature. The composite hydrogel will cross-link immediately in the presence of calcium ions, and the gelation will be complete after 10 min, the composite hydrogel paste was obtained.

Mechanical Properties. Samples used for the tensile test were cut into dumbbells (Figure 2B). The tensile mechanical properties of the composite hydrogel were measured using a universal mechanical testing machine (HengYi Instrument Technology Co., Ltd., Shanghai, China). The prepared sample was clamped at both ends, and the stress−strain curve was determined at a speed of 10 mm/min. The maximum pullout force before failure was defined as the maximum axial pullout strength. The average of at least five tests was reported.

The composite hydrogel was uniaxially compressed with a 1 kN load cell at a cross-head speed of 0.5 mm/min, and stress−strain curves were collected. Maximum stress was taken as compressive strength. Each type of cement was tested at least five times.

Swelling Test. The composite hydrogel was cut into disks with a diameter of 6 mm and a thickness of 2 mm and dried for 24 h at 37 °C in a vacuum oven. Then, the samples were completely immersed in PBS (pH = 7.4) at room temperature, and the solution was replaced at a predefined time. The samples were weighed every 2 h until the mass of the hydrogel did not change obviously.[41] The swelling capacity, M_e, of the composite hydrogel was calculated by the following equation

$$M_e(\%) = (W_t - W_0)/W_0 \times 100$$

where W_t is the weight (g) of the swollen hydrogel at the adsorption time t and W_0 is the initial weight (g) of the composite hydrogel after drying completely.

Morphological Characterization. The composite hydrogel was lyophilized for 24 h. The fracture surface of different composite hydrogel samples was examined for microstructural features by scanning electron microscopy (SEM; Quanta 250; Thermo Fisher Scientific, Waltham, MA, USA).

BSA Loading and Release. The cumulative release curves of bovine serum albumin (BSA) were performed instead of JWH133 because of excellent biocompatibility of BSA, which was used as a drug carrier.[42] BSA (Sigma-Aldrich) was loaded in the control group and in the 4% PAL paste by adding 100 μL of BSA stock solution (c = 10 mg/mL) to 1 g of the paste. To examine the influence of PAL, the release of BSA from these samples was compared with that from a PAL-free paste, which was loaded equivalently. Immediately after loading, the pastes

were cross-linked with a 100 mM $CaCl_2$ solution for 10 min. Samples ($n = 5$) were incubated in 1 mL of PBS at room temperature. The release solution was replaced at certain time points (1, 3, 5, and 7 days), and the amount of BSA in the solution was quantified.

Cell Culture. Bone marrow stem cells (BMSCs) and bone marrow monocytes (BMMs) were acutely isolated from the femoral and tibial bone marrow and cultured in α-MEM containing 10% FBS and 1% penicillin/streptomycin in 5% CO_2 at 37 °C. Nonadherent cells were removed by washing with PBS after 3 days. BMMs were cultured in complete medium with 30 ng/mL of M-CSF. The medium was replaced two to three times a week, and the cells were subcultured using 0.25% trypsin. BMSCs from the third to fifth passages were induced to undergo osteogenic differentiation *in vitro* by culture with osteogenic medium (50 μg/mL ascorbic acid, 0.1 μM dexamethasone and 10 mM β-glycerol-phosphate). The BMMs were cultured with 30 ng/mL of M-CSF and 50 ng/mL of RANKL for osteoclast differentiation.

***In Vitro* Cytocompatibility Test.** Cell viability was measured by the CCK-8 assay according to the manufacturer's instructions. Briefly, cells were seeded in 96-well plates, with five parallel control wells in each group. Then, 10 μL of CCK-8 buffer was added to each well and incubated at 37 °C for 4 h. The OD values at 450 nm were measured by an absorbance microplate reader.

ALP and Alizarin Red S Staining. BMSCs were stained with a BCIP/NBT Alkaline Phosphatase Color Development Kit after 7 days, at the early stages of osteogenic differentiation. Briefly, BMSCs were fixed with 4% paraformaldehyde for 30 min and then stained for 30 min in the dark. The late stage of osteogenic differentiation was investigated after 2 weeks by Alizarin Red S staining. Briefly, the cells were fixed with ethanol for 30 min and then stained for 30 min with Alizarin Red S dye and 5% perchloric acid; the absorbance at 490 nm was determined.

TRAP Staining. BMMs were cultured in 48-well plates at a density of 10^5 cells/well in medium with 30 ng/mL M-CSF and 50 ng/mL RANKL. TRAP staining was performed after 5 days. According to the manufacturer's instructions, the cells were fixed in 37% formaldehyde for 30 min and stained using a Tartaric Phosphate Kit (Sigma-Aldrich, 387A-1KT) for 1 h. TRAP-positive cells were visualized and counted in each well by microscopy.

qRT-PCR. qRT-PCR was performed to evaluate the expression levels of markers during osteoblast and osteoclast formation. BMSCs and BMMs were seeded in 6-well plates at densities of 1×10^4 and 1×10^5 cells/well in induction medium. Then, RNA was extracted using a TRIzol reagent. Next, cDNA was synthesized using Prime Script Reverse Transcriptase Master Mix. qRT-PCR was performed using a real-time PCR system and SYBR Green SuperMix according to the manufacturer's instructions.

Pit Formation Assay. Effect of the composite hydrogel loaded with JWH133 on osteoclast differentiation was determined with 24-well Osteo Assay plates. BMMs were induced with M-CSF and RANKL for 5 days. After the cells were removed, resorption pits were observed by bright-field microscopy, and the percentage of resorbed area was quantified.

Statistical Analysis. All results are expressed as the mean ± standard deviation and were assessed statistically using one-way ANOVA. A *P*-value < 0.05 was considered significant.

RESULTS AND DISCUSSION

Mechanical Properties of the Modified Alginate-Based Composite Hydrogel. The tensile test was performed using a system designed to assess the mechanical strength of the composite hydrogel (Figure 2C). Figure 2D shows the influence of the PAL content on the tensile strength of the composite hydrogel. The addition of PAL dramatically increased the tensile modulus of the composite hydrogel compared to the hydrogel with no PAL. The highest tensile modulus (51.98 ± 4.76 kPa) was observed at a PAL content of 4% (w/v %). The hydrogels with 2% (***$p < 0.001$) and 4% (***$p < 0.001$) PAL both had a significantly higher tensile modulus than the hydrogel with no PAL (11.77 ± 3.64 kPa). Similarly, compression tests were carried out to evaluate the compressive strength of the composite hydrogel. Quantification results are shown in Figure 2E, and 4% PAL (3.65 ± 0.30 MPa) showed the highest compressive strength, higher than 2% (2.12 ± 0.43 MPa, **$p < 0.01$), 1% (**$p < 0.01$) PAL and much higher than the hydrogel with no PAL (0.91 ± 0.04 MPa). The result further indicated that PAL could dramatically increase the mechanical properties of the composite hydrogel.

Hydrogels are ideal vehicles for cell transplantation, but few hydrogels possess the necessary mechanical support strength and osteoconductive characteristics required to integrate with the host bone to accelerate bone formation. PAL is a magnesium aluminum silicate mineral with a hydrated chain-layer structure and has good adsorption ability, as well as good biological activity and compatibility. Bone-associated therapies often require stiff materials, and hydrogels possessing higher elastic moduli are effective for inducing BMSCs toward the osteoblastic lineage. Therefore, the addition of PAL enhanced the mechanical strength of the composite hydrogel, and this improved mechanical support is expected to promote new bone formation.

Swelling Experiments. The swelling ability of the composite hydrogel is important to evaluate. It has been indicated that rapid swelling behavior in scaffolds contributes to cell adsorption and growth. Figure 2F shows the influence of the PAL content on the swelling behavior of the composite hydrogel in PBS (pH = 7.4) at 37 °C. The swelling ratio of the composite hydrogel increased over time. When the PAL content was 4%, the composite hydrogel showed the highest swelling ratio because PAL is also absorbent. In addition, the control sample could not keep its shape in the buffer solution and broke down into small pieces in less than 6 h; thus, the swelling experiment could not be continued for this sample, and this material is not suitable for bone defect repair.

The swelling ratio, which is an indicator of the capacity of hydrogels to imbibe water, was affected by the addition of PAL to the alginate hydrogels. The results indicated that PAL effectively increased the strength of the SA hydrogels and could provide mechanical support. In the SA/PAL system, as the PAL content increased, the swollen composite hydrogels could maintain their shape for a longer time and showed better mechanical support; these changes corresponded to the elastic modulus values of the SA hydrogels upon the addition of hyaluronate. This result can be attributed to the good water absorption characteristics of PAL, as well as its ability to maintain the original shape without substantial deformation while expanding because of water absorption. The swelling properties observed here are suitable for clinical applications,
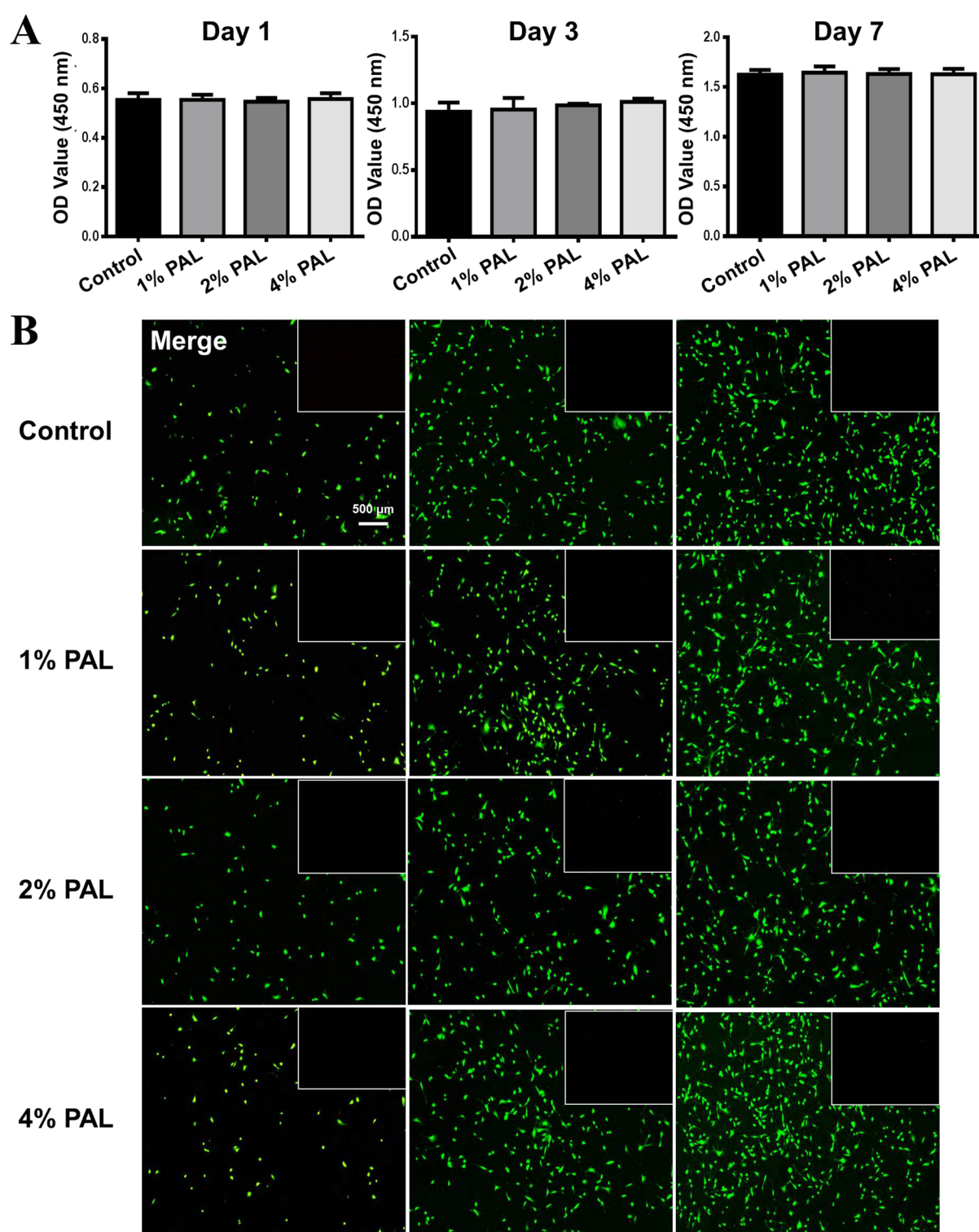
Figure 3. Biocompatibility of the composite hydrogel. (A) Cell proliferation after 1, 3, and 7 days incubation with composite hydrogels with different PAL contents (no PAL, 1, 2, and 4 w/v % PAL group). (B) Fluorescence micrographs of live/dead staining of cells in contact with the composite hydrogels (no PAL, 1, 2, and 4 w/v % PAL group) after 1, 3, and 7 days of incubation. (Green: live cells; Red: dead cells).

not only to fill the defect site but also to provide better mechanical support.

Biocompatibility of the Modified Alginate-Based Composite Hydrogel. First, CCK-8 assays were used to assess the effect of the modified alginate-based hydrogel on the viability of BMSCs. The results of the CCK-8 test showed that after 1, 3, and 7 days of culture, BMSCs proliferated well in the composite hydrogels compared with hydrogels without PAL (Figure 3A) and that the proliferation of BMSCs was not affected by the modified alginate-based hydrogel, with no significant difference among the sample groups. The results also confirmed that the addition of PAL had no effect on the biocompatibility of the SA hydrogels, which confirmed that PAL is nontoxic and has good biocompatibility.
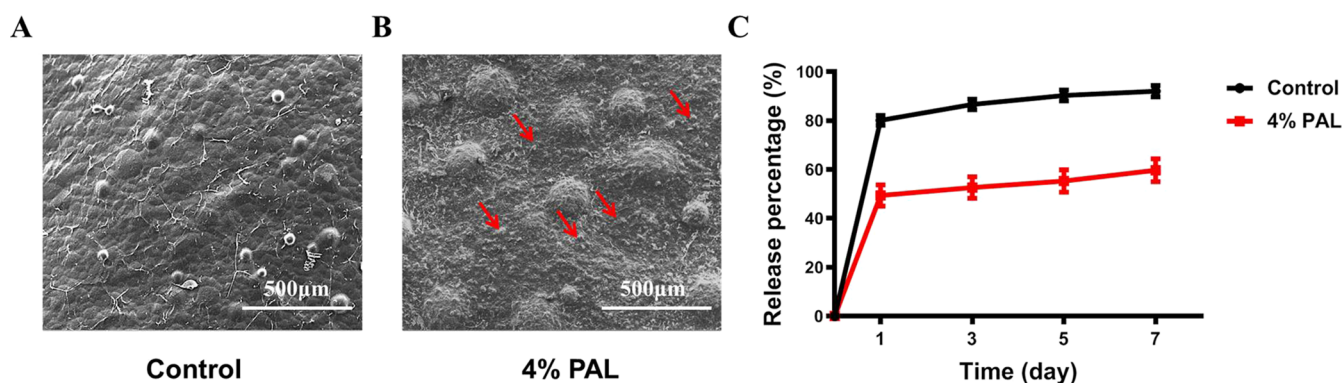
Figure 4. Morphological characterization and cumulative release curves of the composite hydrogels. (A) SEM images showing the morphology of the fracture surface in the control group and (B) 4% PAL group. (C) Cumulative release curves of BSA. The control group showed a high initial burst, while the 4% PAL group demonstrated slower release. The data suggest that a significant amount of BSA remained inside the 4% PAL group samples after 7 days.
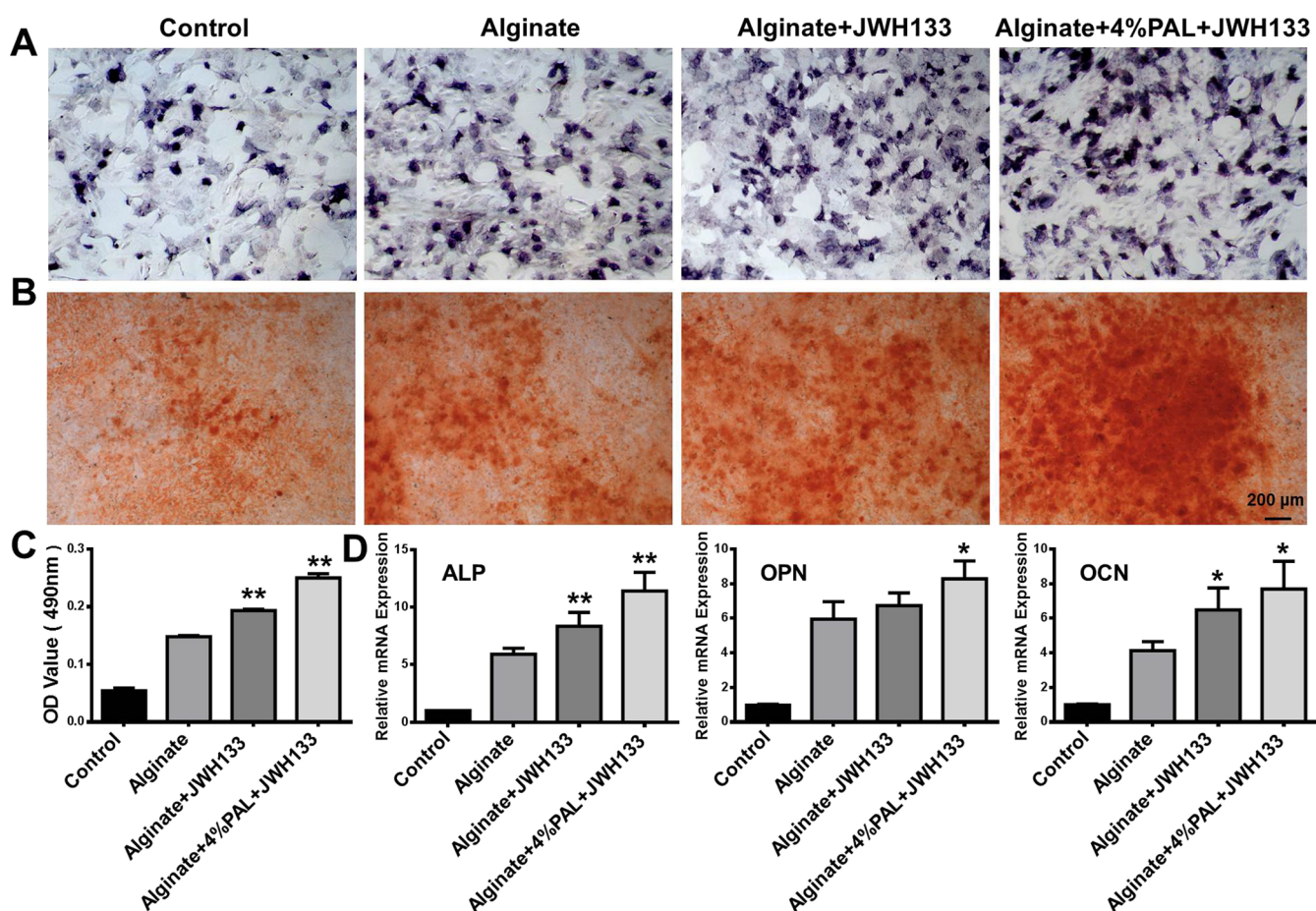

Figure 5. Modified alginate-based hydrogel loaded with JWH133 promotes osteogenic differentiation in BMSCs. (A) Representative images of ALP staining after 7 days. (B) Representative images of ALP staining after 14 days. (C) Quantification of Alizarin Red S staining. (D) Relative mRNA expression of the osteoblast-specific genes ALP, OPN, and OCN. *$P < 0.05$ and **$P < 0.01$ vs the alginate group.

In addition, the results of live/dead staining assays after 1, 3, and 7 days of culture were used to detect the effect on cell viability (Figure 3B). There was no significant difference between the modified alginate-based hydrogel and control groups at the same time point. With prolonged culture time, the number of cells increased obviously, and the cells showed better activity. These results show that the modified alginate-based hydrogel is a biocompatible material suitable for bone regeneration and could show slightly better compatibility with cells than the original hydrogel in vivo. Moreover, Mg^{2+} and Si^{4+} released from PAL endow the composite hydrogels with a good osteoinductive ability.

The SA hydrogel with added PAL showed a slightly better function in promoting cell adhesion growth and promoting proliferation. This difference may be attributed to the adsorption properties of PAL, which is conducive to cells adhering to the surface of the material. In addition, PAL has a nanostructure and a large specific surface area that make it easy
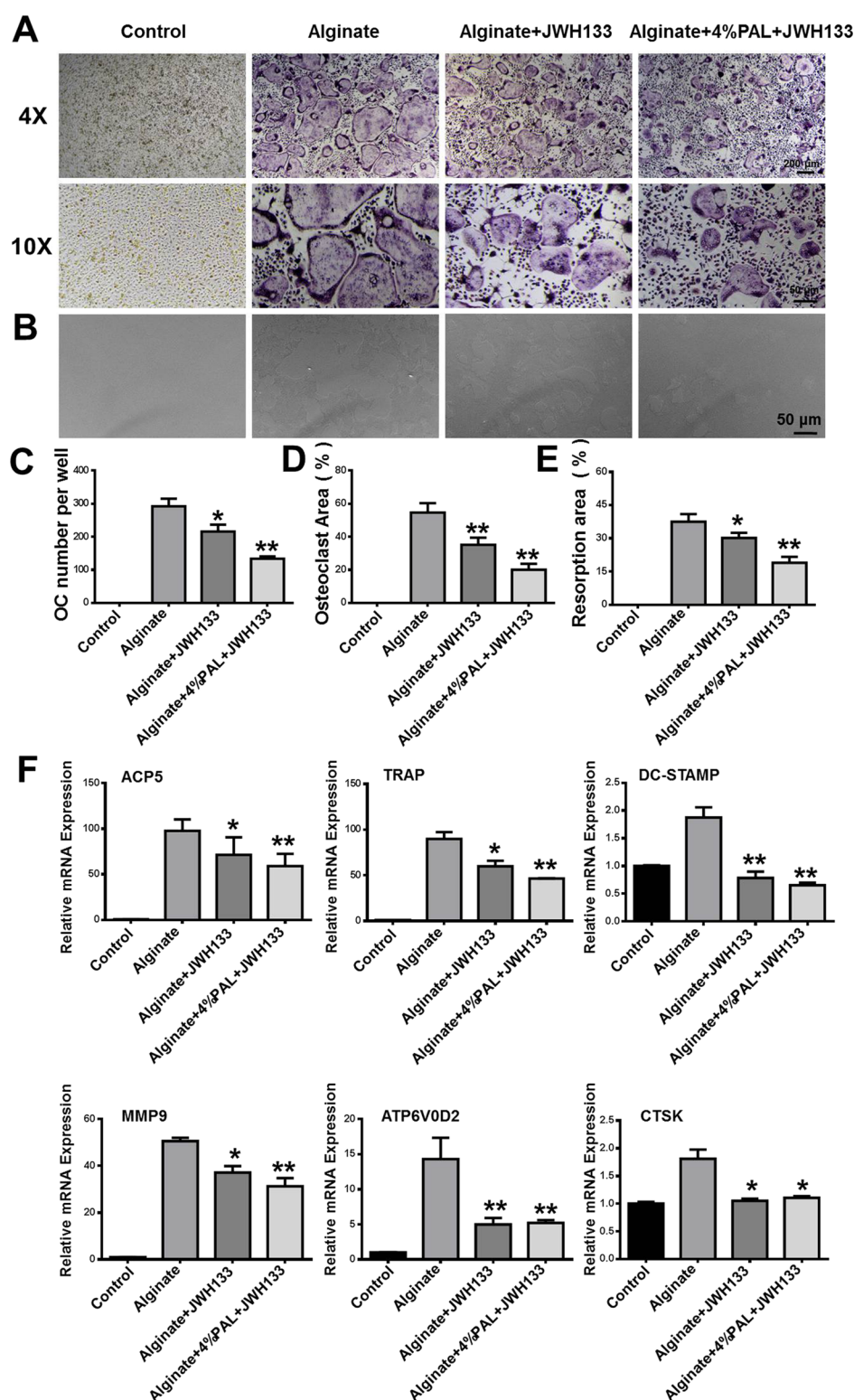
Figure 6. Modified alginate-based hydrogel loaded with JWH133 suppresses RANKL-induced osteoclastogenesis *in vitro*. (A) Representative images of TRAP-positive multinuclear cells after 5 days. (B) Representative images of the resorbed area after 7 days. (C,D) Quantification of TRAP-positive multinuclear cells and the area of osteoclasts. (E) Quantification of the resorbed area after 7 days. (F) Relative mRNA expression of osteoclast-specific genes, including ACP5, TRAP, DC-STAMP MMP9, ATP6V0D2, and CTSK. *$P < 0.05$ and **$P < 0.01$ *vs* the alginate group.

for the cells to exchange nutrients and metabolites in the material, accelerating the growth and proliferation of the cells.

Morphological Characterization. SEM of the novel SA/PAL composite hydrogel (4% PAL) in comparison with the pure SA hydrogel was performed to study the influence of PAL on the

microstructure of the composite hydrogel strands. The pure SA hydrogel revealed a smooth surface according to the primary membrane that is immediately formed by contact with the calcium chloride solution (Figure 4A). In contrast, the SA/PAL composite hydrogel showed an increased surface roughness and

covered with PAL nanoparticles (referring to the red arrow of Figure 4B). Moreover, it was clearly observed that the surface features of the composite hydrogel were interconnected after cross-linking with Ca^{2+}; the original rod-like structure of PAL was covered with sodium alginate after cross-linking, indicating that the modified alginate-based hydrogel was successfully obtained.

BSA Release Kinetics. The BSA-loaded SA/PAL composite hydrogel (4% PAL) and PAL-free paste were incubated in PBS to evaluate the release behavior of BSA. In general, the cumulative release of BSA from the 4% PAL composite hydrogel was lower than that from the PAL-free hydrogel (Figure 4C). The rate of BSA release from the hydrophilic pure SA hydrogel was faster than that from the composite hydrogel, and the cumulative release of BSA reached approximately 90% within 7 days. The rate of BSA release from the 4% PAL composite hydrogel reached approximately 60% because PAL shows good adsorption and delays drug release.

Modified Alginate-Based Composite Hydrogel Loaded with JWH133 Promoted the Osteogenic Differentiation of BMSCs. BMSCs play a major role in tissue engineering and regenerative medicine owing to their self-renewal, multidirectional differentiation, and low immunogenicity. The ability of the composite hydrogel to promote the early osteogenic differentiation of BMSCs was investigated by ALP staining and ALP activity determination. The results show increased ALP expression in the modified alginate-based hydrogel group *in vitro* on day 7 (Figure 5A). Furthermore, calcium deposition was detected by Alizarin Red S staining after 14 days as an indicator of osteogenic activity. The level of calcium deposition was higher in the modified alginate-based hydrogel group than in the alginate-based hydrogel and control groups (Figure 5B,C), showing that the modified alginate-based hydrogel improved the bioactivity of osteogenesis in the later stage. More importantly, the mRNA expression levels of the osteoblast-specific markers ALP, OPN, and OCN were significantly increased in the modified alginate-based hydrogel group, as evaluated by qRT-PCR (Figure 5D). The modified alginate-based hydrogel upregulated osteogenesis-related genes and decreased ALP activity and calcium deposition, possibly because PAL is rich in many elements related to bone formation.

Modified Alginate-Based Hydrogel Loaded with JWH133 Suppresses RANKL-induced Osteoclastogenesis *In Vitro*. Osteoclasts, which are giant multinucleated cells that form from the macrophage lineage, are responsible for resorbing bone and releasing mineral matrix. BMMs were cultured with the control and untreated alginate-based hydrogels loaded with JWH133 and modified alginate-based hydrogels loaded with JWH133 and stimulated with RANKL for 5 days to induce osteoclast activity (Figure 6A). The modified alginate-based hydrogel loaded with JWH133 inhibited the number and area of osteoclasts, as shown by TRAP staining (Figure 6C,D). We next examined the expression of osteoclast-specific genes, including ACP5, TRAP, MMP9, ATP6V0D2, DC-STAMP, and CTSK. The results show that the osteoclast-specific gene expression was upregulated in BMMs stimulated with RANKL. However, the expression was suppressed by JWH133 and further suppressed by the modified alginate-based hydrogel loaded with JWH133 (Figure 6F). This may be because these genes are related to the number, differentiation, and function of osteoclasts. Furthermore, Osteo Assay plates were used to determine whether the modified alginate-based hydrogel loaded with JWH133 could suppress osteoclastic bone

resorption. As shown in Figure 6B,E, the extent of resorption was significantly reduced because of the alginate-based hydrogel loaded with JWH133, particularly, the modified alginate-based hydrogel. Collectively, the result suggests that the modified alginate-based hydrogel loaded with JWH133 suppressed osteoclast differentiation and function *in vitro*. The osteoclast-related assay and bone resorption assay showed that modified alginate-based hydrogels are a biocompatible carrier for JWH133, which is a potentially novel therapy for the treatment of osteoporosis and osteoporotic bone disease.

Same with the results of the attapulgite monomer, we observed the gene expression of our composite hydrogel to promote osteogenic correlation factors and indicated that it has the ability of osteogenicity. Meanwhile, there are some limitations in this study. Because attapulgite is composed of complex inorganic salts, we did not show the potential signaling pathways. We speculate that signaling pathways activated by attapulgite are extensive and lack specificity. Therefore, we are committed to further research on the molecular mechanism to screen accurate signaling pathways.

■ CONCLUSIONS

In this study, we constructed a modified alginate-based hydrogel with a high drug-loading capacity and biocompatibility. Compared to the original alginate hydrogel, the composite hydrogel showed better mechanical properties and similar biocompatibility. In addition, the composite hydrogel loaded with JWH133 stimulated BMSC differentiation into osteoblasts but suppressed osteoclast formation and function *in vitro*. This novel system may have potential as a drug carrier for the treatment of osteoporosis and osteoporotic bone defects in novel future clinical applications.

■ AUTHOR INFORMATION

Corresponding Authors

Meng Li — *Department of Orthopedics, The First Affiliated Hospital of University of Science and Technology of China, Hefei 230001, People's Republic of China;* ⓞ orcid.org/0000-0002-8071-7321; Email: zhuchena@ustc.edu.cn

Chen Zhu — *Department of Orthopedics, The First Affiliated Hospital of University of Science and Technology of China, Hefei 230001, People's Republic of China;* Email: limengustc@163.com

Authors

Wei Zhou — *Department of Orthopedics, The First Affiliated Hospital of University of Science and Technology of China, Hefei 230001, People's Republic of China*

Qianming Li — *Department of Orthopedics, The First Affiliated Hospital of University of Science and Technology of China, Hefei 230001, People's Republic of China*

Ruixiang Ma — *Department of Orthopedics, The First Affiliated Hospital of University of Science and Technology of China, Hefei 230001, People's Republic of China*

Wei Huang — *Department of Orthopedics, The First Affiliated Hospital of University of Science and Technology of China, Hefei 230001, People's Republic of China*

Xianzuo Zhang — *Department of Orthopedics, The First Affiliated Hospital of University of Science and Technology of China, Hefei 230001, People's Republic of China*

Yingsheng Liu — *Department of Orthopedics, The First Affiliated Hospital of University of Science and Technology of China, Hefei 230001, People's Republic of China*

Ze Xu − *Department of Orthopedics, The First Affiliated Hospital of University of Science and Technology of China, Hefei 230001, People's Republic of China*

Linlin Zhang − *Department of Orthopedics, The First Affiliated Hospital of University of Science and Technology of China, Hefei 230001, People's Republic of China*

Complete contact information is available at:
https://pubs.acs.org/10.1021/acsomega.0c06057

Author Contributions

Notes

The authors declare no competing financial interest.

■ ACKNOWLEDGMENTS

■ REFERENCES

(1) Vallet-Regí, M.; Ruiz-Hernández, E. Bioceramics: From Bone Regeneration to Cancer Nanomedicine. *Adv. Mater.* **2011**, *23*, 5177−5218.

(2) Huang, Y.; Zhang, X.; Wu, A.; Xu, H. An injectable nano-hydroxyapatite (n-HA)/glycol chitosan (G-CS)/hyaluronic acid (HyA) composite hydrogel for bone tissue engineering. *RSC Adv.* **2016**, *6*, 33529−33536.

(3) Villate-Beitia, I.; Truong, N. F.; Gallego, I.; Zárate, J.; Puras, G.; Pedraz, J. L.; Segura, T. Hyaluronic acid hydrogel scaffolds loaded with cationic niosomes for efficient non-viral gene delivery. *RSC Adv.* **2018**, *8*, 31934−31942.

(4) Shen, G.-Y.; Ren, H.; Tang, J.-J.; Qiu, T.; Zhang, Z.-D.; Zhao, W.-H.; Yu, X.; Huang, J.-J.; Liang, D.; Yao, Z.-S.; Yang, Z.-D.; Jiang, X.-B. Effect of osteoporosis induced by ovariectomy on vertebral bone defect/fracture in rat. *Oncotarget* **2017**, *8*, 73559−73567.

(5) Chen, X.; Zhao, Y.; Geng, S.; Miron, R. J.; Zhang, Q.; Wu, C.; Zhang, Y. In vivo experimental study on bone regeneration in critical bone defects using PIB nanogels/boron-containing mesoporous bioactive glass composite scaffold. *Int. J. Nanomed.* **2015**, *10*, 839−846.

(6) Yingjie, H.; Ge, Z.; Yisheng, W.; Ling, Q.; Hung, W. Y.; Kwoksui, L.; Fuxing, P. Changes of microstructure and mineralized tissue in the middle and late phase of osteoporotic fracture healing in rats. *Bone* **2007**, *41*, 631−638.

(7) Thormann, U.; Khawassna, T. E.; Ray, S.; Duerselen, L.; Kampschulte, M.; Lips, K.; Von Dewitz, H.; Heinemann, S.; Heiss, C.; Szalay, G.; Langheinrich, A. C.; Ignatius, A.; Schnettler, R.; Alt, V. Differences of bone healing in metaphyseal defect fractures between osteoporotic and physiological bone in rats. *Injury* **2014**, *45*, 487−493.

(8) Beil, F. T.; Barvencik, F.; Gebauer, M.; Seitz, S.; Rueger, J. M.; Ignatius, A.; Pogoda, P.; Schinke, T.; Amling, M. Effects of Estrogen on Fracture Healing in Mice. *J. Trauma: Inj., Infect., Crit. Care* **2010**, *69*, 1259−1265.

(9) Cho, J. S.; Chan Kang, Y. Advanced yolk−shell hydroxyapatite for bone graft materials: kilogram-scale production and structure-in vitro bioactivity relationship. *RSC Adv.* **2014**, *4*, 25234.

(10) Ai, C.; Cai, J.; Zhu, J.; Zhou, J.; Jiang, J.; Chen, S. Effect of PET graft coated with silk fibroin via EDC/NHS crosslink on graft-bone healing in ACL reconstruction. *RSC Adv.* **2017**, *7*, 51303−51312.

(11) Wang, P.; Li, Y.; Jiang, M. Effects of the multilayer structures on Exenatide release and bioactivity in microsphere/thermosensitive hydrogel system. *Colloids Surf., B* **2018**, *171*, 85−93.

(12) Yegappan, R.; Selvaprithiviraj, V.; Mohandas, A.; Jayakumar, R. Nano polydopamine crosslinked thiol-functionalized hyaluronic acid hydrogel for angiogenic drug delivery. *Colloids Surf., B* **2019**, *177*, 41−49.

(13) Deng, L.; Liu, Y.; Yang, L.; Yi, J.-Z.; Deng, F.; Zhang, L.-M. Injectable and bioactive methylcellulose hydrogel carrying bone mesenchymal stem cells as a filler for critical-size defects with enhanced bone regeneration. *Colloids Surf., B* **2020**, *194*, 111159.

(14) Kolk, A.; Handschel, J. R.; Drescher, W.; Rothamel, D.; Kloss, F.; Blessmann, M.; Heiland, M.; Wolff, K. D.; Smeets, R. Current trends and future perspectives of bone substitute materials−From space holders to innovative biomaterials. *J. Craniomaxillofac Surg* **2012**, *40*, 706−718.

(15) Paderni, S.; Terzi, S.; Amendola, L. Major bone defect treatment with an osteoconductive bone substitute. *Musculoskelet. Surg.* **2009**, *93*, 89−96.

(16) Winterbottom, J.; Kaes, D. R.; Tunc, D. C.; Boyce, T. M.; Knaack, D.; Russell, J.; Bhattacharyya, S. Injectable and moldable bone substitute materials. U.S. Patent WO 2007,0847,25A3 2015.

(17) Luckanagul, J. A.; Metavarayuth, K.; Feng, S.; Maneesaay, P.; Clark, A. Y.; Yang, X.; García, A. J.; Wang, Q. Tobacco Mosaic Virus Functionalized Alginate Hydrogel Scaffolds for Bone Regeneration in Rats with Cranial Defect. *ACS Biomater. Sci. Eng.* **2016**, *2*, 606−615.

(18) Maisani, M.; Sindhu, K. R.; Fenelon, M.; Siadous, R.; Rey, S.; Mantovani, D.; Chassande, O. Prolonged delivery of BMP-2 by a non-polymer hydrogel for bone defect regeneration. *Drug Delivery Transl. Res.* **2018**, *8*, 178−190.

(19) Selmi, T. A. S.; Verdonk, P.; Chambat, P.; Dubrana, F.; Potel, J.-F.; Barnouin, L.; Neyret, P. Autologous chondrocyte implantation in a novel alginate-agarose hydrogel: Outcome at Two Years. *J. Bone Jt. Surg.* **2008**, *90*, 597−604.

(20) Lee, K. Y.; Mooney, D. J. Alginate: Properties and biomedical applications. *Prog. Polym. Sci.* **2012**, *37*, 106−126.

(21) Venkatesan, J.; Bhatnagar, I.; Manivasagan, P.; Kang, K.-H.; Kim, S.-K. Alginate composites for bone tissue engineering: A review. *Int. J. Biol. Macromol.* **2015**, *72*, 269−281.

(22) Pawar, S. N.; Edgar, K. J. Alginate derivatization: a review of chemistry, properties and applications. *Biomaterials* **2012**, *33*, 3279−3305.

(23) Abdal-Hay, A.; Sheikh, F. A.; Lim, J. K. Air jet spinning of hydroxyapatite/poly(lactic acid) hybrid nanocomposite membrane mats for bone tissue engineering. *Colloids Surf., B* **2013**, *102*, 635−643.

(24) Lü, L.; Deegan, A.; Musa, F.; Xu, T.; Yang, Y. The effects of biomimetically conjugated VEGF on osteogenesis and angiogenesis of MSCs (human and rat) and HUVECs co-culture models. *Colloids Surf., B* **2018**, *167*, 550−559.

(25) Wang, Y.; Cui, W.; Chou, J.; Wen, S.; Sun, Y.; Zhang, H. Electrospun nanosilicates-based organic/inorganic nanofibers for potential bone tissue engineering. *Colloids Surf., B* **2018**, *172*, 90−97.

(26) Liu, D.; Zheng, H. Enhanced adsorption of radioactive strontium ions from aqueous solution by H2O2-modified attapulgite. *J. Radioanal. Nucl. Chem.* **2017**, *311*, 1883−1890.

(27) Zhao, X.-F.; Liu, Z.-L.; Li, X.-D.; Li, S.-P.; Song, F.-G. The performance of attapulgite hybrids combined with MTX and Au nanoparticles. *J. Phys. Chem. Solids* **2018**, *124*, 73−80.

(28) Anirudhan, T. S.; Divya, P. L.; Nima, J. Synthesis and characterization of novel drug delivery system using modified chitosan based hydrogel grafted with cyclodextrin. *Chem. Eng. J.* **2016**, *284*, 1259−1269.

(29) Zhao, H.; Zhang, X.; Zhou, D.; Weng, Y.; Qin, W.; Pan, F.; Lv, S.; Zhao, X. Collagen, polycaprolactone and attapulgite composite scaffolds for in vivo bone repair in rabbit models. *Biomed. Mater.* **2020**, *15*, 045022.

(30) Zou, X.; Pan, J.; Ou, H.; Wang, X.; Guan, W.; Li, C.; Yan, Y.; Duan, Y. Adsorptive removal of Cr(III) and Fe(III) from aqueous solution by chitosan/attapulgite composites: Equilibrium, thermodynamics and kinetics. *Chem. Eng. J.* **2011**, *167*, 112−121.

(31) Wang, Z.; Zhao, Y.; Luo, Y.; Wang, S.; Zhang, L.; Shi, X. Electrospun attapulgite-doped poly(lactic-co-glycolic acid) nanofibers for osteogenic differentiation of human mesenchymal stem cells. *J. Controlled Release* **2015**, *213*, No. e146.

(32) An, J.; Yang, H.; Zhang, Q.; Liu, C.; Zhao, J.; Zhang, L.; Chen, B. Natural products for treatment of osteoporosis: The effects and mechanisms on promoting osteoblast-mediated bone formation. *Life Sci.* **2016**, *147*, 46.

(33) Zhang, H.; Zheng, L.; Yuan, Z. Lycium barbarum polysaccharides promoted proliferation and differentiation in osteoblasts. *J. Cell. Biochem.* **2018**, *120*, 5018−5023.

(34) Huang, Y.; Yin, Y.; Gu, Y.; Gu, Q.; Shi, Q. Characterization and immunogenicity of bone marrow-derived mesenchymal stem cells under osteoporotic conditions. *Sci. China Life Sci.* **2020**, *63*, 429−442.

(35) Xiao, W.; Li, S.; Pacios, S.; Wang, Y.; Graves, D. T. Bone Remodeling Under Pathological Conditions. *Front. Oral Biol.* **2016**, *18*, 17.

(36) Zhang, Y.; Rohatgi, N.; Veis, D. J.; Schilling, J.; Teitelbaum, S. L.; Zou, W. PGC1β Organizes the Osteoclast Cytoskeleton by Mitochondrial Biogenesis and Activation. *J. Bone Miner. Res.* **2018**, *33*, 1114−1125.

(37) Guindon, J.; Hohmann, A. G. Cannabinoid CB2 receptors: a therapeutic target for the treatment of inflammatory and neuropathic pain. *Br. J. Pharmacol.* **2008**, *153*, 319−334.

(38) Ofek, O.; Attar-Namdar, M.; Kram, V.; Dvir-Ginzberg, M.; Mechoulam, R.; Zimmer, A.; Frenkel, B.; Shohami, E.; Bab, I. CB2 cannabinoid receptor targets mitogenic Gi protein−cyclin D1 axis in osteoblasts. *J. Bone Miner. Res.* **2011**, *26*, 308−316.

(39) Sophocleous, A.; Landao-Bassonga, E.; van't Hof, R. J.; Idris, A. I.; Ralston, S. H. The type 2 cannabinoid receptor regulates bone mass and ovariectomy-induced bone loss by affecting osteoblast differentiation and bone formation. *Endocrinology* **2011**, *152*, 2141−2149.

(40) Zhu, M.; Yu, B.; Bai, J.; Wang, X.; Guo, X.; Liu, Y.; Lin, J.; Hu, S.; Zhang, W.; Tao, Y. Cannabinoid receptor 2 agonist prevents local and systemic inflammatory bone destruction in rheumatoid arthritis. *J. Bone Miner. Res.* **2019**, *34*, 739−751.

(41) Zuo, R.; Meng, L.; Guan, X.; Wang, J.; Yang, J.; Lin, Y. Removal of strontium from aqueous solutions by acrylamide-modified attapulgite. *J. Radioanal. Nucl. Chem.* **2019**, *319*, 1207−1217.

(42) Yu, M.; Duan, X.; Cai, Y.; Zhang, F.; Jiang, S.; Han, S.; Shen, J.; Shuai, X. Multifunctional Nanoregulator Reshapes Immune Microenvironment and Enhances Immune Memory for Tumor Immunotherapy. *Adv. Sci.* **2019**, *6*, 1900037.